THIRD YEAR LABORATORY

AN INTRODUCTION TO RADIO TELESCOPES AND PULSAR ASTRONOMY

The experiment takes places on Tuesdays. The location where you will conduct the experiment is alternating from week to week between Jodrell Bank Observatory and Manchester. Some groups have their first lab day in Jodrell Bank Observatory, while others start in Manchester. Whether you start in Jodrell Bank Observatory or Manchester will get allocated by the 3rd year lab tutor.

This experiment has a significant computer programming component in python.

1 Aims

In this experiment we learn about the basics of radio astronomy and then combine this knowledge with computer programming to investigate radio pulsars. Depending on if you start in Jodrell Bank Observatory, or Manchester, the order in which you complete sub-parts can be different. Discuss this with your demonstrator.

Part 1: Introduction to radio telescopes and pulsar observing. You will learn to operate the 42-ft radio telescope at Jodrell Bank Observatory. With this telescope you will observe several pulsars and record pulses as a function of observing frequency. You will write a computer program to calculate the “dispersion measure” to the pulsar and hence estimate its distance.

Part 2: Searching for radio pulsars. You will use some existing data obtained with the 76-m Lovell radio telescope to search for the presence of a radio pulsar and to measure its period. To do this, you will write a programme and use simple Fourier analysis techniques.

Part 3: Timing the Crab pulsar. You will use data obtained with the 42-ft telescope on the ‘Crab pulsar’ to measure pulse arrival times at the observatory over a period of a few days. These times must be corrected to the barycentre of the Solar System to obtain an accurate period of the star and you will establish how this period evolves over time. This entails writing a third computer program to analyse and correct the arrival time data. From your results the age and surface magnetic field of the neutron star in the Crab Nebula can be deduced.

2 Objectives

1. Use the 42-ft radio telescopes to measure the dispersion measure and therefore distance to several pulsars.
2. Write a computer program to determine the period of unknown pulsars using the Fourier transform.
3. Write a computer program to accurately determine the period and period derivative of the Crab pulsar.

Safety Notice
The observing room at Jodrell Bank Observatory contains many pieces of unfamiliar equipment. Do not touch any equipment unless instructed. Be mindful of trip hazards, equipment and cables may be temporarily located on the floor.
You must attend a mandatory site safety briefing on Tuesday morning of your first lab day at Jodrell Bank (first or second week of the lab block depending on what start location you got allocated) before starting the experiment.

3 Background reading

Some suggestions for background reading:

- Background information about pulsars is given in the article by Lorimer "Radio Pulsars: An Observer's Perspective" and a more detailed review which both can be found online[1].
- See `http://www.jb.man.ac.uk/research/pulsar/Education/`
- Textbook "Handbook of Pulsar Astronomy" by Duncan Lorimer and Michael Kramer
- Textbook "Pulsar Astronomy" by Lyne & Graham-Smith

4 An Introduction to Radio Telescopes

In this experiment you will operate the 13-m "42-ft" radio telescope and also work with data recorded using the 76-m Lovell telescope. These are prime-focus reflecting radio telescopes, and as such you should ensure you have an understanding of the optics and signal processing you rely upon when using these instruments.

4.1 Optics

The primary reflecting surface of such a telescope is a paraboloid of revolution which focusses the incoming radiation onto a 'feed' aerial (see Fig. 1). Its action is, therefore, to turn plane waves into spherical waves whose centre of curvature is at the primary focus. In order to maximise the efficiency of the telescope, power reflected from near the edges of the dish must be collected by the feed. However, in so doing unwanted power will also be picked up from the surroundings of the telescope; this is termed 'spillover'. The response of the feed as a function of direction is therefore tailored to maximise the ratio between the 'gain' of the telescope and the overall system noise temperature to which the spillover contributes (see below).

4.2 Signal processing

The incoming electromagnetic radiation induces an oscillating potential difference in the feed, which can be thought of as an AC electrical signal which is then transmitted via coaxial cable. In order to turn the incoming oscillating voltage into useful scientific data, the signal goes through various stages, including amplification, filtering, mixing, attenuation and finally digitisation. The digitised signal is then further processed with digital electronics such as FPGAs, general purpose computers or dedicated digital signal processing hardware.

[1] Radio Pulsars: An Observer's Perspective:
`http://www.jb.man.ac.uk/research/pulsar/lab/lorimer99.pdf`
Detailed review: `https://arxiv.org/pdf/astro-ph/0104388.pdf`

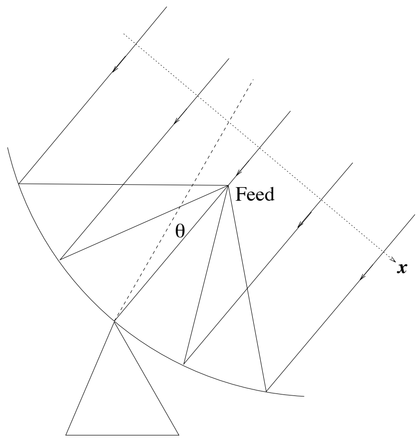

Figure 1: Schematic diagram of a radio telescope

The 42-ft telescope is equipped with a heterodyne receiver as shown in Figure 2. The noise-like signals are collected by the telescope over a range of frequencies of the electromagnetic radiation. In the case of the 42-ft telescope the recorded data will have a bandwidth of 10 MHz centred at a frequency of 611 MHz. The collected signals are 'mixed' with a pure sinusoidal local oscillator (LO) signal. This process causes the voltage waves to interfere and create both sum and difference frequencies.

$$f_{\rm diff} = f_{\rm RF} - f_{\rm LO} \qquad f_{\rm sum} = f_{\rm RF} + f_{\rm LO},$$

where $f_{\rm RF}$ corresponds to the frequency of the collected electromagnetic radiation (in the range of 606 MHz and 616 MHz). A filter is used to keep only the difference signals, i.e. the lower frequencies $f_{\rm diff}$, which are more convenient for passing along long lengths of cable from the focus box to the observing room.

After reaching the observing room, the voltage is measured with a digitiser, and passed into a computer for further processing. In radio astronomy, we are often interested in the amplitude of the signal as a function of frequency, so we use a digital filterbank to split the signal into fine frequency channels. The digital filterbank works by taking a small segment of the voltage data and computing a Fourier transform to generate 40 frequency channels. The power in each frequency channel is computed by squaring the amplitude of the resultant complex numbers. This gives us a measurement of power as a function of frequency every $2\,\mu{\rm s}$ (this is $\frac{40}{2\times 10\,{\rm MHz}}$, can you explain why?). In order to reduce the data volume and increase the signal-to-noise ratio, we integrate over time by summing the powers for each channel. For observations of known pulsars, we can compute a histogram of power vs pulse phase (rotational phase of the star) for each frequency channel by computing the pulse phase of a given $2\,\mu{\rm s}$ time sample and adding the corresponding power to the appropriate phase bin.

4.3 Pulsar observing with the 42-ft Radio Telescope

Pulsars were discovered in 1967 by Bell & Hewish at Cambridge. Within a year it was accepted that they were rotating neutron stars. The 76-m Lovell telescope, as well as the 42-ft telescope, are more flexible instruments for studying known pulsars and for finding new ones than the dipole array used by Bell & Hewish. A significant part of the subsequent detective work on pulsars has therefore been carried out at Jodrell Bank.

Speak to your demonstrator about how to drive the telescope.

Once you have been approved by the demonstrator, observe the pulsar B0329+54.

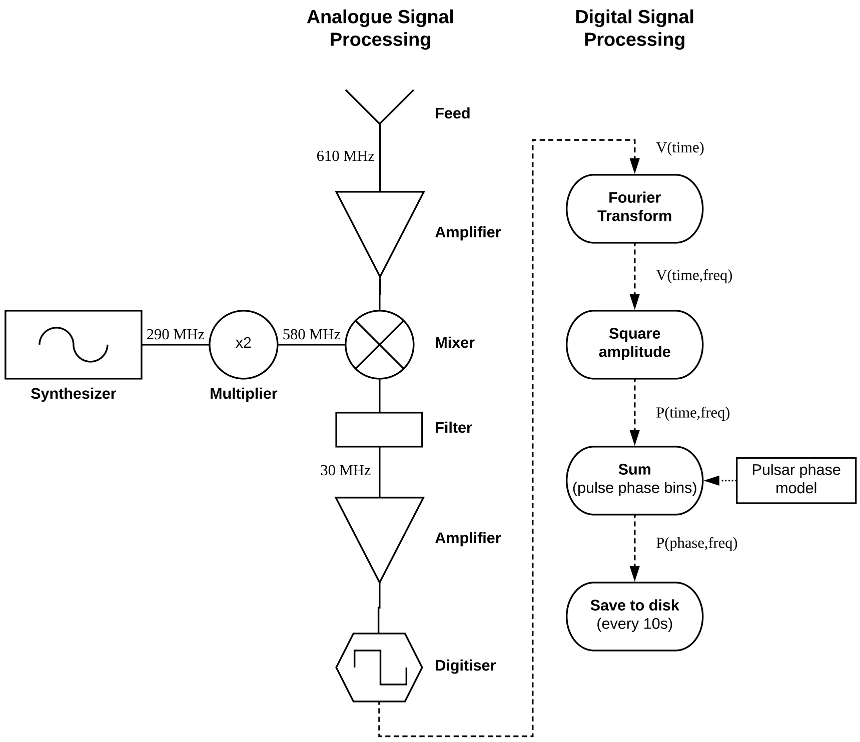

Figure 2: Schematic diagram of the heterodyne receiver and digital filterbank

Make sure you can see and understand the plots output by the telescope software.

4.4 Calibration and Noise Temperature

Essentially all the signals we deal with in radio astronomy are composed of random noise. The parameter most often used to characterise these signals is the 'noise temperature', T (measured in K) which is directly proportional to *mean noise power* available from a resistor at temperature T. From the theorem of equipartition of energy there are $kT/2$ Joules of energy associated with each 'degree of freedom' of the system, i.e. in each Hz and in each of the two polarisation states. Thus the power per unit bandwidth is kT Watts Hz^{-1} and over a bandwidth B Hz the total power available is kTB Watts. Absolute calibration measurements in radio astronomy are therefore made using 'hot and cold loads' which are resistors at well-defined temperatures (e.g. liquid He, liquid N and room temperature).

After amplification, the random noise signals, which have a zero mean, are turned into a more useful form by a *detector*. Usually in radio astronomy we use a device (most simply based on a diode operating on the bottom part of its characteristic curve) which responds to the square of the input voltage i.e. to the power of the random signal integrated over an appropriate period. In a basic receiver this period could be set by an RC 'time constant'. Because the statistical nature of the input signal there is a *random fluctuating* component in the detected signal (see Fig. 2) whose magnitude is $\propto T/\sqrt{B\tau}$ where τ is the time over which the signal is averaged. (Note that this is akin to the fluctuations $\propto \sqrt{N}$ in Poisson statistics). Thus the accuracy of the measurement of the mean power is increased by increasing the signal bandwidth and the averaging time.

The total noise power at the output of the receiver, often called the 'system noise temperature' $T_{\rm sys}$, has several contributions:

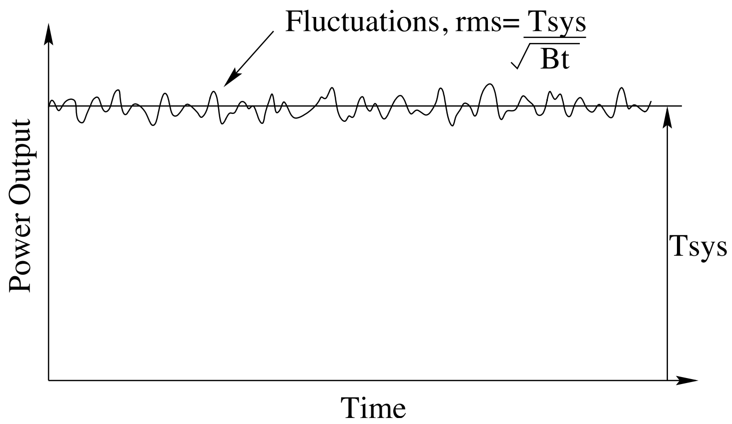

Figure 3: The noisy signal after square-law detection

i) $T_{\rm source}$, the desired contribution coming from the radio source.

ii) $T_{\rm sky}$, the contribution from the sky around the source.

iii) $T_{\rm spillover}$, the contribution from the ground around the telescope.

iv) $T_{\rm rec}$, the noise generated in the receiver electronics.

Because we are dealing with random noise signals the powers add i.e.

$$T_{\rm sys} = T_{\rm source} + T_{\rm sky} + T_{\rm spillover} + T_{\rm rec}.$$

For these observations $T_{\rm rec} \approx 100{\rm K}$, $T_{\rm sky} \approx 20{\rm K}$ and $T_{\rm spillover} \approx 10{\rm K}$.

The relationship between the flux density received from sources on the sky and the equivalent noise temperature is characterised by the telescope's *gain* (sensitivity) usually expressed in units K/Jy. Note that 1 Jy corresponds to 10^{-26} W m^{-2} Hz^{-1} and that it is a measure of the power falling on unit area per unit bandwidth. The gain is given by

$$G = \frac{\eta A}{2k},$$

where A is the physical area of the telescope and η is the 'aperture efficiency', a factor which accounts for blockages or tapering of the beam shape to avoid spillover. The aperture efficiency of the 42-ft telescope is $\sim 55\%$ (i.e its effective collecting area is 55% of its physical area).

Use the information in this section to compute the gain of the 42-ft telescope in K/Jy.

Show that the system equivalent flux density, i.e. the flux density that would induce an increase in system temperature by the rms fluctuations in T, is given by:

$$S_{\rm SEFD} = \frac{T_{\rm sys}}{G\sqrt{n_p B\tau}}$$

where n_p is the number of polarisations that have been summed.

What would be the minimum integration time required to detect a 1 Jy source with the 42-ft radio telescope?

When observing pulsars, we can take advantage of the repeating signal to average each pulse in phase. This increases our signal-to-noise ratio by a factor of $\sqrt{(P-W)/W}$, where P is the pulsar period and W is the pulse width.

Use the equations in this section and values from Appendix E to compute the signal-to-noise ratio you would expect for your observation of PSR B0329+54. How does it compare with your observed signal-to-noise ratio?

Use the list of pulsars in Appendix E to plan observations of other pulsars. Think about how long you would need to integrate and when the pulsar is visible from Jodrell Bank. Carry out your planned observations.

You should aim to understand what Celestial coordinates are and how they are related to local sidereal time. You may find it helpful to consult an astronomy textbook. You may want to refer to the Jodrell Bank Internet Observatory website[2], which gives you the elevation of the source as function time.

You will use these observations in the next part of the experiment, so make sure to record high signal-to-noise ratio observations of at least 2 or 3 pulsars.

4.5 Measurement of pulsar dispersion measures

On its way to the Earth the pulsed radiation passes through ionised plasma in the interstellar medium (ISM). The refractive index of plasma is a function of frequency and hence the radiation experiences a frequency dependent delay – i.e. the ISM is dispersive. From the difference in arrival time as a function of frequency one can calculate the 'dispersion measure', the integrated electron number density along the line-of-sight to the pulsar i.e.

$$DM = \int_{\mathrm{pulsar}}^{\mathrm{earth}} n_e \cdot \mathrm{d}l.$$

More details about the frequency dispersion in pulse arrival time are given in Appendix D. The dispersive effect of the ISM causes initially sharp pulses to become smeared in addition to suffering an overall delay, when observed with a receiver with a finite bandwidth.

In this part of the experiment, you will write a computer program to visualise and process your data files. Ask your demonstrator how to access the template programs and the data files[3]. You're strongly encouraged to use google colab to do the programming, as this gives access to your work using just a browser. This is particularly useful given your work location alternates between JBO and Manchester.

Write a computer program to:

i) **Visualise the pulse intensity as a function of phase and frequency,**

ii) **De-disperse the data for a given DM, and average over frequency,**

iii) **Measure the DM for each of your pulsars.**

You will need to use the relevant equation in Appendix D to determine the DM of the pulsars. Think about how you will estimate the error on your measurements.

Assuming a value of the mean electron density in the ISM of 0.03 cm^{-3} calculate the distance of the pulsars. Compare your value with the published value.

5 Detection of an unknown pulsar and measurement of its period

One of the greatest challenges in pulsar astronomy is the discovery of pulsars of unknown periodicity. Only once the period is known can the pulsar data be "folded" to produce high

[2] `http://webmail.jb.man.ac.uk/distance/observatory/index.php`

[3] At time of writing, data can be obtained from `https://psrweb.jb.man.ac.uk/lab/42ft/`

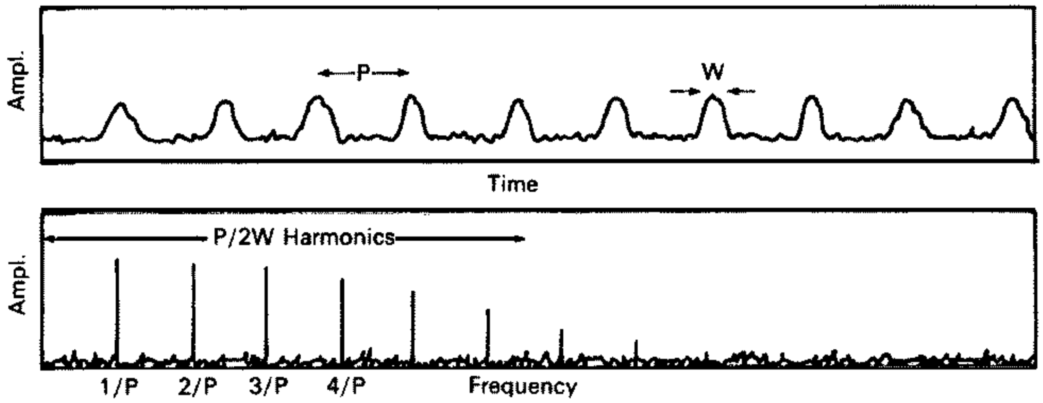

Figure 4: The spectrum of a sequence of pulses from a pulsar, taken from Fig. 3.3 of "Pulsar Astronomy" by Lyne and Smith (1998).

signal-to-noise ratio profiles which can be used to study the pulsar in detail.

This search process is now carried out by inspection of the power spectrum of the data which will show delta functions at the fundamental rotation frequency of the pulsar and its harmonics, the number of harmonics being roughly equal to $P/2W$, where P is pulse period and W is the pulse width (see figure 3). From the frequency of the Nth harmonic, $\nu_{\rm N}$, the frequency of the fundamental can be estimated as $\nu_{\rm N}/{\rm N}$.

Write a computer program to perform the Fourier transform of a time sequence of samples obtained with the 76-m Lovell radio telescope (ask your lab demonstrator for a template for the computer code and data).

By graphical inspection of the resultant amplitude spectrum (obtained by calculating the amplitude of each of the complex numbers in the spectrum), estimate the frequency and width of the pulses in the time sequence. Think about the uncertainty in your frequency determination for the different harmonics and how to obtain the most accurate result.

6 Pulse arrival times from the Crab Pulsar

Much can be inferred about the physics of neutron stars and their binary companions (if present) from an analysis of the precise arrival times of the pulses. You will measure a set of profiles obtained with the 42-ft telescope, on the powerful pulsar in the Crab Nebula. The data should ideally be taken on at least two separate days with a gap of several days between them.

It is straightforward to determine the raw arrival times (defined as the time the pulse arrives after the beginning of the observation) from your data using the provided python template. The arrival times produced by the template code will be given in Modified Julian Date[4], and an error will be given in seconds. In this part of the experiment you will write a computer program to determine the period of the pulsar for each of your observations.

Before one can use these data for physical interpretation they must be corrected for the motion of the observatory around the Sun, i.e. the pulse train should appear to have been collected at a fixed point in space. The most convenient point to use is the centre of mass of the Solar System, its *barycentre*.

[4]MJD is the number of days since midnight on November 17, 1858. A convenient value for recording astronomical dates that avoids complications of traditional date formats.

Data on the position of the centre of the Earth with respect to the barycentre are given in the *Astronomical Almanac* and can be obtained as a text file from the 42-ft data portal. However, since positions are only provided once per day, it will be necessary to interpolate between the data points to be able to correct the arrival times to a sufficient precision. The typical error in the arrival time of a pulse in the raw data is ~ 0.2 milliseconds, and the interpolation error must be less than this. An additional correction is required because the observatory is not located at the centre of the Earth! It has a very simple form: $r\sin(\epsilon)/c$, where r is the radius of the Earth, ϵ is the elevation of the source above the horizon and c is the velocity of light.

Justify the form of the Earth-telescope correction with a simple diagram.

Draw a diagram which demonstrates the principles of the barycentric correction.

Write a computer program to:

i) **Perform the interpolation between the barycentre positions using one of the Lagrange multi-point formulas (see Appendix C) after determining which one is suitable.**

ii) **Correct for the light travel times from the Earth's centre to the Solar System barycentre.**

iii) **Make the further correction for the observatory displacement from the centre of the Earth.**

A template programme is provided.

Your program should now be able to correct the measured pulse arrival times to the solar system barycentre. You will need to adapt your program to accurately measure the period of the Crab pulsar from these data.

Your data files include a suitable initial period estimate for the Crab pulsar on the days of your observations - this will be your initial model period. It can be useful to think of the pulse arrival times in terms of a number of rotations of the star, which can be trivially estimated using a model period, P, using

$$N = \frac{t - t_0}{P},$$

Where t is the pulsar arrival time t_0 is your reference epoch. If your model period were correct, each arrival time would correspond to an integer number of rotations of the star. In the case your model period is not correct you will observe a fractional remainder when dividing the arrival time by the model period. This remainder is the difference between the true pulse arrival time and your model of the pulse arrival time, and is known as the residual.

Think about how the residual will vary with time when the true period and model period are slightly different. It may help you to sketch a train of pulses and think what happens when you compare it to a model with a slightly incorrect period. The residual will change in a systematic way, and this behaviour can be used to compute a new estimate of the pulsar period.

Make a prediction of how the residual will vary as a function of time and determine how to compute a new period estimate from the residuals.

Adapt your computer program to calculate the residuals for an input period, and plot the residual as a function of time.

Make sure you understand the form of the plot you have produced. If the plot does not match your expectation, make sure to consider what assumptions you used when computing the residuals.

Use the residuals to determine an accurate period of the Crab pulsar for each of the two days of data.

Determine the period derivative, and hence estimate the age of the pulsar and its surface magnetic field.

Make sure to quote the errors on your answers!

Appendix A: Observing with the 42-ft telescopes

Please watch the pre-lab videos before starting the lab. Speak to the lab demonstrator before operating the 42-ft telescope, or if you are unsure of any instructions. For later reference, a description of the graphical user interface of the telescope control software is available at
`http://www.jb.man.ac.uk/~undergrd/42ft/`

Once data have been recorded, ask your lab demonstrator to copy it to the notebook server for further processing.

Appendix B: Pulsar analysis software

For the “DM estimation” and “Crab timing” parts of the experiment, the folded pulsar data you are using can be worked on with a scientific software package called *PSRCHIVE*. **The details of reading the raw data are handled by the python template code you are given.**

The jupyter notebook server should have the following template codes:

Simple Plotter Simple Plotter is a simple code that demonstrates how to plot data using matplotlib and numpy

Pulsar Data Viewing and Dispersion Measure This is a template for the first part of the experiment. You can use it to visualise your pulsar observations and then adapt it to measure the dispersion measure

List Data This is a tool that can quickly list out all the data in your directories, and print header information from those. This will be useful for the first part of the experiment.

Searching for Pulsars This is a template for the second part of the experiment (The “FFT” part). Here you can read Lovell telescope observations and use the Fourier transform to find periodic signals from pulsars. In this part you will read raw time-series data from the Lovell telescope, which are stored as 8-bit signed integers (numpy data type is `np.int8`) and can e.g. be read with the `fromfile` function in numpy. There is a separate plain-text header file for each data file.

Make Time of Arrivals This notebook is a more-or-less complete tool to extract ”ToAs” from your observations of the Crab pulsar. The ToA (Time of Arrival) is a measurement of the time at which a pulse of a pulsar is recorded. This ToA is the reference time of the observation plus an offset which describes how long you had to wait after the start of the measurement to record the first pulse. This code also provides a function to get the approximate spin period of the crab pulsar at the time of the observation.

Crab Pulsar Timing This is a template for the final part of the experiment. You will need to write code to correct the ToAs to the solar-system barycentre and to accurately measure the period of the Crab pulsar.

A note on the data format The raw data for the “DM estimation” and “Crab timing” are a 3-d “data cube” of intensity as a function of pulse phase, time and frequency. For every frequency channel, a histogram of intensity as a function of pulse phase is recorded for a set amount of time (usually around 1 minute). In your experiment you are provided with files that have averaged to about 10 minutes per time step to reduce the data volume, and converted to numpy data files for ease of reading into the python codes.

25. Numerical Interpolation, Differentiation, and Integration

Numerical analysts have a tendency to accumulate a multiplicity of tools each designed for highly specialized operations and each requiring special knowledge to use properly. From the vast stock of formulas available we have culled the present selection. We hope that it will be useful. As with all such compendia, the reader may miss his favorites and find others whose utility he thinks is marginal.

We would have liked to give examples to illuminate the formulas, but this has not been feasible. Numerical analysis is partially a science and partially an art, and short of writing a textbook on the subject it has been impossible to indicate where and under what circumstances the various formulas are useful or accurate, or to elucidate the numerical difficulties to which one might be led by uncritical use. The formulas are therefore issued together with a caveat against their blind application.

Formulas

Notation: Abscissas: $x_0<x_1<\ldots$; functions: $f, g, \ldots$; values: $f(x_i)=f_i$, $f'(x_i)=f_i'$. $f', f^{(2)}, \ldots$ indicate 1st, 2d, … derivatives. If abscissas are equally spaced, $x_{i+1}-x_i=h$ and $f_p=f(x_0+ph)$ (p not necessarily integral). R, R_n indicate remainders.

25.1. Differences

Forward Differences

25.1.1

$$\Delta(f_n)=\Delta_n=\Delta_n^1=f_{n+1}-f_n$$

$$\Delta_n^2=\Delta_{n+1}^1-\Delta_n^1=f_{n+2}-2f_{n+1}+f_n$$

$$\Delta_n^3=\Delta_{n+1}^2-\Delta_n^2=f_{n+3}-3f_{n+2}+3f_{n+1}-f_n$$

$$\Delta_n^k=\Delta_{n+1}^{k-1}-\Delta_n^{k-1}=\sum_{j=0}^{k}(-1)^j\binom{k}{j}f_{n+k-j}$$

Central Differences

25.1.2

$$\delta(f_{n+\frac12})=\delta_{n+\frac12}=\delta_{n+\frac12}^1=f_{n+1}-f_n$$

$$\delta_n^2=\delta_{n+\frac12}^1-\delta_{n-\frac12}^1=f_{n+1}-2f_n+f_{n-1}$$

$$\delta_{n+\frac12}^3=\delta_{n+1}^2-\delta_n^2=f_{n+2}-3f_{n+1}+3f_n-f_{n-1}$$

$$\delta_n^{2k}=\sum_{j=0}^{2k}(-1)^j\binom{2k}{j}f_{n+k-j}$$

$$\delta_{n+\frac12}^{2k+1}=\sum_{j=0}^{2k+1}(-1)^j\binom{2k+1}{j}f_{n+k+1-j}$$

$\delta_{\frac12 n}^k=\Delta_{\frac12(n-k)}^k$ if n and k are of same parity.

Forward Differences

$$\begin{array}{cccccc}
x_0 & f_0 & & & \\
 & & \Delta_0 & & \\
x_1 & f_1 & & \Delta_0^2 & \\
 & & \Delta_1 & & \Delta_0^3 \\
x_2 & f_2 & & \Delta_1^2 & \\
 & & \Delta_2 & & \\
x_3 & f_3 & & &
\end{array}$$

Central Differences

$$\begin{array}{cccccc}
x_{-1} & f_{-1} & & & \\
 & & \delta_{-\frac12} & & \\
x_0 & f_0 & & \delta_0^2 & \\
 & & \delta_{\frac12} & & \delta_{\frac12}^3 \\
x_1 & f_1 & & \delta_1^2 & \\
 & & \delta_{3/2} & & \\
x_2 & f_2 & & &
\end{array}$$

Mean Differences

25.1.3 $\mu(f_n)=\frac12(f_{n+\frac12}+f_{n-\frac12})$

Divided Differences

25.1.4 $[x_0,x_1]=\dfrac{f_0-f_1}{x_0-x_1}=[x_1,x_0]$

$$[x_0,x_1,x_2]=\frac{[x_0,x_1]-[x_1,x_2]}{x_0-x_2}$$

$$[x_0,x_1,\ldots,x_k]=\frac{[x_0,\ldots,x_{k-1}]-[x_1,\ldots,x_k]}{x_0-x_k}$$

Divided Differences in Terms of Functional Values

25.1.5 $[x_0,x_1,\ldots,x_n]=\displaystyle\sum_{k=0}^{n}\frac{f_k}{\pi_n'(x_k)}$

25.1.6 where $\pi_n(x)=(x-x_0)\,(x-x_1)\ldots(x-x_n)$ and $\pi_n'(x)$ is its derivative:

25.1.7

$$\pi_n'(x_k)=(x_k-x_0)\ldots(x_k-x_{k-1})(x_k-x_{k+1})\ldots(x_k-x_n)$$

Let D be a simply connected domain with a piecewise smooth boundary C and contain the points $z_0,\ldots,z_n$ in its interior. Let $f(z)$ be analytic in D and continuous in $D+C$. Then,

25.1.8 $[z_0,z_1,\ldots,z_n]=\dfrac{1}{2\pi i}\displaystyle\int_C\frac{f(z)}{\prod_{k=0}^{n}(z-z_k)}dz$

25.1.9 $\Delta_0^n=h^nf^{(n)}(\xi)\qquad(x_0<\xi<x_n)$

25.1.10

$$[x_0,x_1,\ldots,x_n]=\frac{\Delta_0^n}{n!h^n}=\frac{f^{(n)}(\xi)}{n!}\qquad(x_0<\xi<x_n)$$

25.1.11

$$[x_{-n},x_{-n+1},\ldots,x_0,\ldots,x_n]=\frac{\delta_0^{2n}}{h^{2n}(2n)!}$$

Reciprocal Differences

25.1.12

$$\rho(x_0,x_1)=\frac{x_0-x_1}{f_0-f_1}$$

$$\rho_2(x_0,x_1,x_2)=\frac{x_0-x_2}{\rho(x_0,x_1)-\rho(x_1,x_2)}+f_1$$

$$\rho_3(x_0,x_1,x_2,x_3)=\frac{x_0-x_3}{\rho_2(x_0,x_1,x_2)-\rho_2(x_1,x_2,x_3)}+\rho(x_1,x_2)$$

$\cdot$

$\cdot$

$$\rho_n(x_0,x_1,\ldots,x_n)=\frac{x_0-x_n}{\rho_{n-1}(x_0,\ldots,x_{n-1})-\rho_{n-1}(x_1,\ldots,x_n)}+\rho_{n-2}(x_1,\ldots,x_{n-1})$$

25.2. Interpolation

Lagrange Interpolation Formulas

25.2.1 $f(x)=\displaystyle\sum_{i=0}^{n}l_i(x)f_i+R_n(x)$

25.2.2

$$l_i(x)=\frac{\pi_n(x)}{(x-x_i)\pi_n'(x_i)}=\frac{(x-x_0)\ldots(x-x_{i-1})(x-x_{i+1})\ldots(x-x_n)}{(x_i-x_0)\ldots(x_i-x_{i-1})(x_i-x_{i+1})\ldots(x_i-x_n)}$$

Remainder in Lagrange Interpolation Formula

25.2.3

$$R_n(x)=\pi_n(x)\cdot[x_0,x_1,\ldots,x_n,x]=\pi_n(x)\cdot\frac{f^{n+1}(\xi)}{(n+1)!}\qquad(x_0<\xi<x_n)$$

25.2.4

$$|R_n(x)|\leq\frac{(x_n-x_0)^{n+1}}{(n+1)!}\max_{x_0\leq x\leq x_n}|f^{(n+1)}(x)|$$

25.2.5

$$R_n(z)=\frac{\pi_n(z)}{2\pi i}\int_C\frac{f(t)}{(t-z)(t-z_0)\ldots(t-z_n)}dt$$

The conditions of **25.1.8** are assumed here.

Lagrange Interpolation, Equally Spaced Abscissas

n Point Formula

25.2.6 $f(x_0+ph)=\displaystyle\sum_k A_k^n(p)f_k+R_{n-1}$

For n even, $\left(-\frac12(n-2)\leq k\leq\frac12 n\right)$.

For n odd, $\left(-\frac12(n-1)\leq k\leq\frac12(n-1)\right)$.

25.2.7

$$A_k^n(p)=\frac{(-1)^{\frac12n+k}}{\left(\frac{n-2}{2}+k\right)!(\frac12n-k)!(p-k)}\prod_{t=1}^{n}(p+\tfrac12n-t)\qquad n\text{ even.}$$

$$A_k^n(p)=\frac{(-1)^{\frac12(n-1)+k}}{\left(\frac{n-1}{2}+k\right)!\left(\frac{n-1}{2}-k\right)!(p-k)}\prod_{t=0}^{n-1}\left(p+\frac{n-1}{2}-t\right),\qquad n\text{ odd.}$$

25.2.8

$$R_{n-1}=\frac{1}{n!}\prod_k(p-k)h^nf^{(n)}(\xi)\approx\frac{1}{n!}\prod_k(p-k)\Delta_0^n\qquad(x_0<\xi<x_n)$$

k has the same range as in **25.2.6**.

Lagrange Two Point Interpolation Formula (Linear Interpolation)

25.2.9 $f(x_0+ph)=(1-p)f_0+pf_1+R_1$

25.2.10 $R_1(p)\approx.125h^2f^{(2)}(\xi)\approx.125\Delta^2$

Lagrange Three Point Interpolation Formula

25.2.11

$$f(x_0+ph)=A_{-1}f_{-1}+A_0f_0+A_1f_1+R_2$$
$$\approx\frac{p(p-1)}{2}f_{-1}+(1-p^2)f_0+\frac{p(p+1)}{2}f_1$$

25.2.12

$$R_2(p)\approx .065h^3f^{(3)}(\xi)\approx .065\Delta^3 \qquad (|p|\leq 1)$$

Lagrange Four Point Interpolation Formula

25.2.13

$$f(x_0+ph)=A_{-1}f_{-1}+A_0f_0+A_1f_1+A_2f_2+R_3$$
$$\approx\frac{-p(p-1)(p-2)}{6}f_{-1}+\frac{(p^2-1)(p-2)}{2}f_0$$
$$-\frac{p(p+1)(p-2)}{2}f_1+\frac{p(p^2-1)}{6}f_2$$

25.2.14 $\qquad R_3(p)\approx$

$$.024h^4f^{(4)}(\xi)\approx .024\Delta^4 \qquad (0<p<1)$$
$$.042h^4f^{(4)}(\xi)\approx .042\Delta^4 \qquad (-1<p<0,\ 1<p<2)$$
$$(x_{-1}<\xi<x_2)$$

Lagrange Five Point Interpolation Formula

25.2.15

$$f(x_0+ph)=\sum_{i=-2}^{2}A_if_i+R_4$$
$$\approx\frac{(p^2-1)p(p-2)}{24}f_{-2}-\frac{(p-1)p(p^2-4)}{6}f_{-1}$$
$$+\frac{(p^2-1)(p^2-4)}{4}f_0-\frac{(p+1)p(p^2-4)}{6}f_1$$
$$+\frac{(p^2-1)p(p+2)}{24}f_2$$

25.2.16 $\qquad R_4(p)\approx$

$$.012h^5f^{(5)}(\xi)\approx .012\Delta^5 \qquad (|p|<1)$$
$$.031h^5f^{(5)}(\xi)\approx .031\Delta^5 \qquad (1<|p|<2) \qquad (x_{-2}<\xi<x_2)$$

Lagrange Six Point Interpolation Formula

25.2.17

$$f(x_0+ph)=\sum_{i=-2}^{3}A_if_i+R_5$$
$$\approx\frac{-p(p^2-1)(p-2)(p-3)}{120}f_{-2}$$
$$+\frac{p(p-1)(p^2-4)(p-3)}{24}f_{-1}$$
$$-\frac{(p^2-1)(p^2-4)(p-3)}{12}f_0$$
$$+\frac{p(p+1)(p^2-4)(p-3)}{12}f_1-\frac{p(p^2-1)(p+2)(p-3)}{24}f_2$$
$$+\frac{p(p^2-1)(p^2-4)}{120}f_3$$

25.2.18 $\qquad R_5(p)\approx$

$$.0049h^6f^{(6)}(\xi)\approx .0049\Delta^6 \qquad (0<p<1)$$
$$.0071h^6f^{(6)}(\xi)\approx .0071\Delta^6 \qquad (-1<p<0,\ 1<p<2)$$
$$.024h^6f^{(6)}(\xi)\approx .024\Delta^6 \qquad (-2<p<-1,\ 2<p<3)$$
$$(x_{-2}<\xi<x_3)$$

Lagrange Seven Point Interpolation Formula

25.2.19 $\qquad f(x_0+ph)=\sum_{i=-3}^{3}A_if_i+R_6$

25.2.20

$$R_6(p)\approx\begin{cases} .0025h^7f^{(7)}(\xi)\approx .0025\Delta^7 & (|p|<1)\\ .0046h^7f^{(7)}(\xi)\approx .0046\Delta^7 & (1<|p|<2)\\ .019h^7f^{(7)}(\xi)\approx .019\Delta^7 & (2<|p|<3)\end{cases}$$
$$(x_{-3}<\xi<x_3)$$

Lagrange Eight Point Interpolation Formula

25.2.21 $\qquad f(x_0+ph)=\sum_{i=-3}^{4}A_if_i+R_7$

25.2.22

$$R_7(p)\approx\begin{cases} .0011h^8f^{(8)}(\xi)\approx .0011\Delta^8 & (0<p<1)\\ .0014h^8f^{(8)}(\xi)\approx .0014\Delta^8 & (-1<p<0)\ (1<p<2)\\ .0033h^8f^{(8)}(\xi)\approx .0033\Delta^8 & (-2<p<-1)\ (2<p<3)\\ .016h^8f^{(8)}(\xi)\approx .016\Delta^8 & (-3<p<-2)\ (3<p<4)\end{cases}$$
$$(x_{-3}<\xi<x_4)$$

Aitken's Iteration Method

Let $f(x|x_0, x_1, \ldots, x_k)$ denote the unique polynomial of k^{th} degree which coincides in value with $f(x)$ at $x_0, \ldots, x_k$.

25.2.23

$$f(x|x_0,x_1)=\frac{1}{x_1-x_0}\begin{vmatrix} f_0 & x_0-x\\ f_1 & x_1-x\end{vmatrix}$$

$$f(x|x_0,x_2)=\frac{1}{x_2-x_0}\begin{vmatrix} f_0 & x_0-x\\ f_2 & x_2-x\end{vmatrix}$$

$$f(x|x_0,x_1,x_2)=\frac{1}{x_2-x_1}\begin{vmatrix} f(x|x_0,x_1) & x_1-x\\ f(x|x_0,x_2) & x_2-x\end{vmatrix}$$

$$f(x|x_0,x_1,x_2,x_3)=\frac{1}{x_3-x_2}\begin{vmatrix} f(x|x_0,x_1,x_2) & x_2-x\\ f(x|x_0,x_1,x_3) & x_3-x\end{vmatrix}$$

Reaching such a small fraction of the receiver noise level is commonly achieved in radio astronomical observations by using a wide receiver bandwidth B and averaging the signal over an integration time τ. The smallest detectable signal is then a fraction $(B\tau)^{-1/2}$ of the total noise level. Typically, a receiver might have a bandwidth of 1 MHz, and it may be required to detect a single pulse 10 milliseconds long; the sensitivity would then be 10^{-2} of the input noise, or about 1 Jy in a large radio telescope. Single pulses are rarely as strong as 1 Jy, and weaker pulses would be lost in noise. However a series of 10 000 pulses, suitably added together, would provide a further factor of 10^{-2}, giving a more useful sensitivity of 10^{-2} Jy within the averaged pulse; the mean flux density of a detectable pulsar will, of course, be lower than this, depending on the ratio of pulse width to period.

3.2 Frequency dispersion in pulse arrival time

Although the basic characteristic of the pulsar signal which facilitates its recognition is the precise periodicity, a second important characteristic is the frequency dispersion in arrival time due to the ionised interstellar medium. This may assist the recognition of a pulsar signal against locally generated impulsive radio interference, but it also plays an important part in restricting the range of a pulsar search.

Radio pulses travel in the ionised interstellar medium at the group velocity v_g, which for small electron densities is related to the free space velocity c by

$$v_g \simeq c\left(1 - \frac{n_e e^2 \lambda^2}{2\pi m c^2}\right) = c\left(1 - \frac{n_e e^2}{2\pi m \nu^2}\right) \tag{3.1}$$

where n_e is the electron number density and e and m are the electronic charge and mass. Hence the travel time T over distance L is

$$T = \int_0^L \frac{dl}{v_g} \simeq \frac{L}{c} + \frac{e^2 \int_0^L n_e dl}{2\pi m c \nu^2} = \frac{L}{c} + 1.345 \times 10^{-3} \nu^{-2} \int_0^L n_e dl \ \text{ s.} \tag{3.2}$$

The first term here is just the free space travel time and the second is the additional dispersive delay t. Customary units in astrophysics are parsecs (3×10^{18} cm) for distance and cm^{-3} for density: the integral $\int_0^L n_e dl$, which measures the total electron content between the pulsar and the observer, is known as dispersion measure, DM, with units cm^{-3} pc. Observers usually quote radio frequencies in megahertz, so that the delay t becomes

$$t = \frac{\text{DM}}{2.410 \times 10^{-4} \nu_{\text{MHz}}^2} \text{ s.} \tag{3.3}$$

The frequency dependence of this delay has a very important effect on observations of radio pulses. A short broad-band pulse will arrive earlier at higher frequencies, traversing the radio spectrum at a rate

$$\dot{\nu} = -1.205 \times 10^{-4} \frac{\nu_{\text{MHz}}^3}{\text{DM}} \text{ MHz s}^{-1}; \tag{3.4}$$

correspondingly, a receiver with bandwidth B (MHz) will stretch out a short pulse to

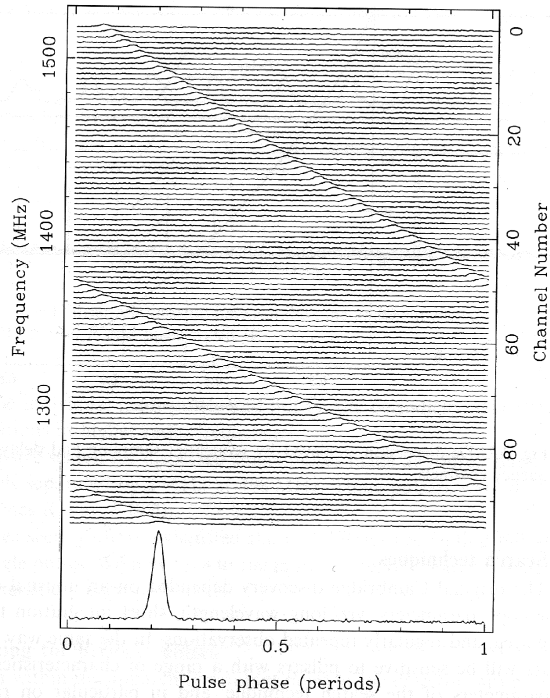

Fig. 3.1. Frequency dispersion in pulse arrival time for PSR B1641−45, recorded in 96 adjacent frequency channels, each 3 MHz wide, centred on 1380 MHz.

a length

$$\Delta t = 8.3 \times 10^3 \mathrm{DM} \nu_{\mathrm{MHz}}^{-3} B \text{ s.} \tag{3.5}$$

As a useful guide, $\Delta t = (202/\nu_{\mathrm{MHz}})^3$ DM milliseconds per MHz bandwidth.

If a pulsar with high dispersion measure is observed with a receiver with a wide bandwidth, its pulse is stretched and the peak intensity is reduced. The lost sensitivity may, however, be recovered by dividing a wide receiver bandwidth into separate bands and using separate receiver channels on each as in Figure 3.1. The output of these separate channels can then be added with appropriate delays so that the pulse components are properly superposed. This process of 'de-dispersion' is shown in Figure 3.2.

The technique first used for 'de-dispersion' involved a mechanically-driven sequential sampling of the separate receiver outputs (Large & Vaughan 1971). Digital techniques are now universally in use, either setting the individual delays to match the known DM of a given pulsar, or using a series of different delays in an off-line search through recorded data. Each set of delays then allows the detection of pulsars in a definite range of DM.

Appendix E: List of Bright Pulsars

A list of bright pulsars, taken from the ATNF Pulsar Catalogue, “psrcat”. Note that flux densities are quoted for 1400 MHz, and you may want to use the typical pulsar spectral index of -1.4 (i.e. $S \propto \nu^{-1.4}$) to correct to your observing frequency.

Name	RA (h:m:s)	Dec (°:′:″)	Period (s)	FWHM (ms)	Flux density (mJy)
B0833-45	08:35:20.6	-45:10:34.8	0.089328	2.100	1100.00
B1641-45	16:44:49.2	-45:59:09.5	0.455060	8.200	296.40
B0329+54	03:32:59.3	+54:34:43.5	0.714520	6.600	203.00
J0437-4715	04:37:15.8	-47:15:09.1	0.005757	0.141	149.00
B0950+08	09:53:09.3	+07:55:35.7	0.253065	9.500	84.00
B0736-40	07:38:32.3	-40:42:40.9	0.374920	29.000	83.70
B1451-68	14:56:00.1	-68:43:39.2	0.263377	12.500	80.00
B1933+16	19:35:47.8	+16:16:39.9	0.358738	9.000	42.00
B1556-44	15:59:41.5	-44:38:45.9	0.257056	6.000	40.00
B2020+28	20:22:37.0	+28:54:23.1	0.343402	12.000	38.00
B1929+10	19:32:13.9	+10:59:32.4	0.226518	7.400	36.00
B1133+16	11:36:03.2	+15:51:04.4	1.187913	31.700	32.00
B2016+28	20:18:03.8	+28:39:54.2	0.557953	14.900	30.00
B2021+51	20:22:49.8	+51:54:50.2	0.529197	7.400	27.00
B0628-28	06:30:49.4	-28:34:42.7	1.244419	58.200	23.00
B0355+54	03:58:53.7	+54:13:13.7	0.156384	3.900	23.00
B1642-03	16:45:02.0	-03:17:58.3	0.387690	4.200	21.00
B1054-62	10:56:25.5	-62:58:47.6	0.422447	20.000	21.00
B2111+46	21:13:24.3	+46:44:08.8	1.014685	32.100	19.00
B1749-28	17:52:58.6	-28:06:37.3	0.562558	9.100	18.00
B2154+40	21:57:01.8	+40:17:45.9	1.525266	38.600	17.00
B1557-50	16:00:53.0	-50:44:20.9	0.192601	5.400	17.00
B1648-42	16:51:48.7	-42:46:11	0.844081	110.000	16.00
B1323-62	13:27:17.4	-62:22:44.6	0.529913	11.000	16.00
B0835-41	08:37:21.1	-41:35:14.3	0.751624	8.900	16.00
B2310+42	23:13:08.6	+42:53:13.0	0.349434	8.800	15.00
B1804-08	18:07:38.0	-08:47:43.2	0.163727	8.900	15.00
B0740-28	07:42:49.0	-28:22:43.7	0.166762	5.400	15.00
B1449-64	14:53:32.7	-64:13:15.5	0.179485	4.400	14.00
B0531+21	05:34:31.9	+22:00:52.0	0.033392	3.000	14.00
B0403-76	04:01:51.6	-76:08:13.8	0.545253	18.000	14.00
B1800-21	18:03:51.4	-21:37:07.3	0.133667	14.000	13.90
J0248+6021	02:48:18.6	+60:21:34.7	0.217094	26.000	13.70
B1937+21	19:39:38.5	+21:34:59.1	0.001558	0.038	13.20
B2045-16	20:48:35.6	-16:16:44.5	1.961572	84.200	13.00

Last updated by : Michael Keith & Patrick Weltevrede on 29 January 2025.

Original version Andrew Lyne and Peter Wilkinson, with modifications from Dunc Lorimer, Patrick Weltevrede, Ben Stappers & Chris Jordan.